# RF Energy Harvesting and Management for Near-zero Power Passive Devices

Yuanfei Huang\*, Akshay Athalye\*, Samir Das<sup>†</sup>, Petar Djurić\* and Milutin Stanaćević\*
\*Department of Electrical and Computer Engineering, Stony Brook University, Stony Brook, NY 11794

†Department of Computer Science, Stony Brook University, Stony Brook, NY 11794

Email: milutin.stanacevic@stonybrook.edu

Abstract—We present RF energy harvester and management strategy tailored for the passive near-zero power devices. Radioless RF-powered backscattering tags that have the ability to recognize and localize activities in the surrounding environment are example of such devices. We propose a management strategy that determines the operation regime of the harvester based on the input power level at which harvester provides the instantaneous supply voltage for device operation. As the input power exceeds this level, the storage of the excess energy is managed by an adaptive capacitor charging circuit that keeps the voltage at the input of voltage regulator constant. We demonstrate that backscatter-based RF tag in the listening mode of operation can instantaneously operate with an input power of -34.4 dBm. Due to the adaptive capacitor charging circuit, the power efficiency of the energy harvester is higher than 50% over a range of input powers from -25 dBm up to -5 dBm.

#### I. INTRODUCTION

The management of the operation of RF energy harvesting near-zero power passive devices with a low capacity energy storage element introduces some unique challenges compared to the energy management in a traditional sensor node. Conventional sensory nodes incorporate active radios that dominate the power budget, although significant steps have been made in reducing their power consumption [1]-[5]. The sensor nodes with energy harvesting have optimized energy-neutral operation that maximizes their performance with the respect to the available energy, either on node-level or application-level [6]-[11]. Backscatter based communication reduces the energy cost of the communication by a few orders of magnitude compared to the sensor node with active radio [12]-[14]. This results in a different energy budget distribution for different modes of operation compared to the conventional sensor node and calls for different management techniques to be used in the implementation of near-zero passive devices, like RF tags [15], that communicate through backscatter. The minimum incident power at which a RF tag can communicate and sense the channel with the instantaneous supply voltage is -30 dBm [16], a power that tag would receive at a distance of around 10 m from an exciter with 1 W emitting power and carrier frequency of 915 MHz.

The incident power at a RF harvesting device depends on a distance to the external RF source and the excitation power, so the harvester has to be able to harvest energy for a wide range of incident RF power. Design of the energy harvester with high energy efficiency over a wide input power range presents significant challenge. In order to tackle the variable nature of the input power, a reconfigurable harvesting system for charging a storage capacitor by the excess harvested energy was proposed [17], [18]. However, the energy management does not detect the low input power when the stored energy can be used for the operation of the device. In [19], the stored energy can be reused and the device can operate at a low input power but it has to charge and discharge the capacitor even when the input power is sufficient for the device to operate. For maintaining a high PCE with a wide input power range, a cascading dc-dc converter is proposed in [20] with a nonlinear time-domain maximum power point tracking (MPPT) method to extract the converted RF power by tuning the load resistance. However, it requires complex analog blocks, such as DC-DC converter which suffers from bulky off-chip passive components. In this work, we propose a novel energy harvester that is managed to efficiently operate with a very wide range of input power leveraging the proposed adaptive charging circuit.

The paper is organized as follows. Section II introduces the architecture and operation of the RF energy harvesting and management circuitry. Section III briefly illustrates the rectifier and the control logic used in the system and describes the design and theoretical analysis of the proposed adaptive capacitor charger with the simulation results presented in Section IV. Conclusions are outlined in Section V.

# II. ENERGY HARVESTING SYSTEM DESCRIPTION

Figure 1 depicts the block diagram of the proposed energy harvesting and management system. The system comprises reconfigurable cross-coupled rectifier, demodulator, low power LDO regulator, adaptive capacitor charger (ACC), control logic, voltage limiter [21] and ultra-low power voltage reference [22]. An off-chip tunable matching (MN) network is used to enable maximum power transfer from the antenna to the input of the rectifier.

We first describe the operation of the energy harvesting and management system. The adaptive structure of the harvester includes reconfigurable rectifier and reconfigurable loading circuit. The harvester senses the input power and the output voltage of the rectifier. The power is sensed in order to adapt the architecture of the rectifier. The power efficiency of a rectifier strongly depends on the input power and the load, with the efficiency maximized in a narrow range of the input

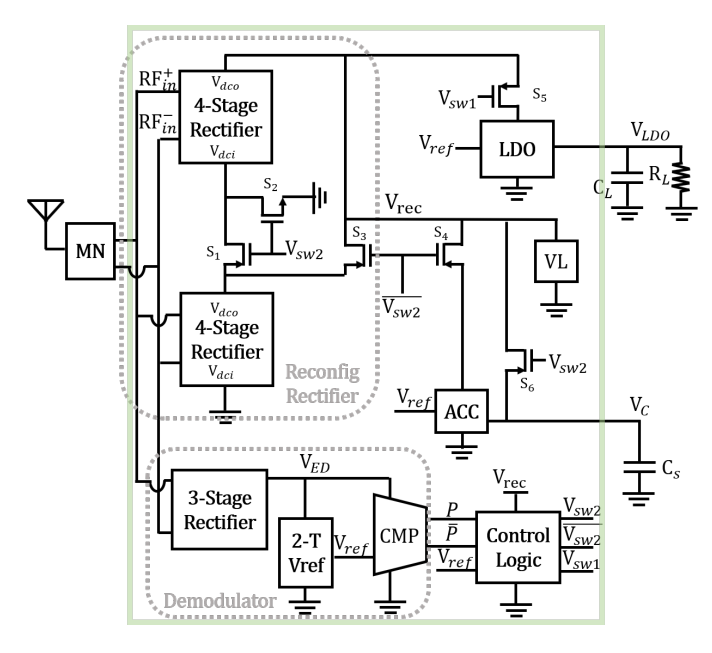


Fig. 1. Block diagram of the proposed RF energy harvesting and management system.

power [23]. The harvester uses reconfigurable rectifier architecture to optimize the power efficiency and the output voltage. The rectifier with higher number of stages at low input power provides the higher power efficiency and output voltage [24]. The power threshold level  $P_{th}$  is set by the minimum power required for the operation of the overall passive device, that is the power at which the voltage regulator can output the required supply voltage. In the presented architecture of the harvester, we use a single threshold power, while a more threshold levels can be added for different operation modes of the passive device with different operating power. The rectifier would then be optimized in terms of energy efficiency for each of these operational modes. For example, in the case of the RF tag, the minimum power is set by the operation of the demodulator circuit that detects the transmission by another tag in the vicinity or the dynamic changes in the environment [15]. Additionally operating modes of RF tag are transmitting, receiving, channel estimation and computation [16].

The system also monitors the output voltage of the rectifier. When the input power is lower than the set power threshold, if the output voltage of the rectifier is lower than a threshold voltage  $V_{th2}$ , the energy harvesting circuit charges the storage element through a single transistor switch. The storage element is chosen to be a film capacitor due to the low leakage [19].  $V_{th2}$  corresponds to the maximum voltage to be stored on the capacitor. Once the output voltage of the rectifier reaches  $V_{th2}$ , the path to the regulator is enabled and the supply voltage for the operation of the tag is provided at the output of the regulator. The storage capacitor  $C_s$  assists rectifier in enabling LDO to output the required supply voltage for the operation of the device. When the capacitor voltage drops below  $V_{th1}$ , LDO is disconnected and the capacitor is charged again.  $V_{th1}$ 

TABLE I 3 STATES OF THE EH SYSTEM.

State	$P_{in}$	$V_{reco}$	$V_{sw1}$	$V_{sw2}$	Rectifier	Load Circuit
1	$< P_{th}$	$< V_{th2}$	0	0	8-stage	charge $C_s$
2	$< P_{th}$	$>V_{th1}$	1	0	8-stage	$LDO$ + discharge $C_s$
3	$>P_{th}$	X	1	1	2x4-stage	LDO+ACC

is selected as the minimum output voltage of the rectifier at which LDO can still output the required supply voltage.

When the input power is higher than the power threshold, LDO is connected to the output of the rectifier. If the voltage at the output of the rectifier is lower than the minimum input voltage of LDO, the pass transistor in ACC is turned off and the output voltage of the rectifier is increasing with LDO as the only load. Once the voltage reaches the minimum input voltage of the rectifier, the pass transistor in ACC turn on. ACC charges the capacitor  $C_s$  with excess energy and keeps the voltage output of the rectifier at the same level by tuning the load of the rectifier. This also maximizes the energy efficiency of the LDO regulator, as the voltage drop across the regulator is maintain at the same level. In the proposed manner, the maximum power efficiency of the overall harvester is maintained over a wide range of the input power. The operation of the tag is summarized in the table I.

#### III. CIRCUIT IMPLEMENTATION

# A. Reconfigurable Rectifier

The incident RF energy at a harvesting device, like RF tag, depends on the distance to the external RF source and the device surrounding. This leads to a wide range of the incident RF power at which the energy harvester has to operate and maintain energy efficiency. The efficiency of a rectifier with a fixed architecture can be optimized only in a narrow range of input power. Adaptive architectures of rectifier that optimize the energy efficiency over a wide range of the incident power have been proposed [18] and we selected the architecture shown in Figure 1. The reconfigurable rectifier consists of two 4-stage rectifiers that can be combined in an 8-stage rectifier and three MOS switches that control the configuration. The 8-stage rectifier is optimized to provide maximum power efficiency at the power threshold level  $P_{th}$ .

# B. Adaptive Capacitor Charger

As the input power exceeds the power dissipated by the tag operation, the excess energy can be saved on a storage element, capacitor. A novel adaptive capacitor charger (ACC) is proposed to control the output voltage of the rectifier by introducing additional load current that charges the storage capacitor. With the ACC, the rectifier holds sufficient output voltage for the LDO to maintain supply voltage for the operation of the tag even if the capacitor voltage is lower than the rectifier output voltage. This warrants a low drop voltage of LDO maintaining a high efficiency of LDO.

The loading resistance of the rectifier has a significant effect on the output voltage,  $V_{rec}$ , as illustrated by a simplified model in Figure 2. The rectifier is modeled by an voltage source

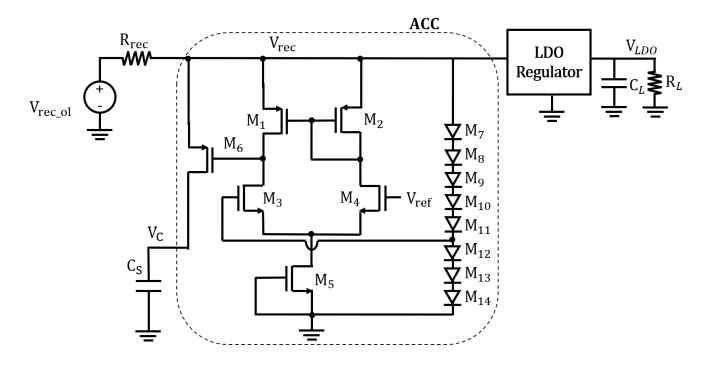


Fig. 2. Model of the proposed energy harvester with the circuit implementation of the adaptive capacitor charger.

 $V_{rec\_ol}$  that corresponds to the output rectifier voltage with no resistive load and equivalent output resistance  $R_{rec}$  [24]. The rectifier loading resistance comprises input resistances of ACC,  $R_{ACC}$  and LDO,  $R_{LDO}$ . Control of  $V_{rec}$  to a desired voltage with different input power can be achieved by tuning  $R_{ACC}$ . Figure 2 also shows the proposed circuit implementation of ACC. The circuit is designed based on conventional LDO design for keeping rectifier output voltage at 0.9 V, leaving 0.1 V drop-out voltage for LDO. It comprises a one-stage differential amplifier as an error amplifier, a MOSdiode based voltage divider  $M_7 \sim M_{14}$ , and a pass-transistor  $M_6$ . The error amplifier compares the divided output voltage with  $V_{ref}$  providing a feedback signal to  $M_6$ . Therefore, when the output voltage of the rectifier is higher than 0.9 V, the gate voltage of  $M_6$ ,  $V_{q6}$ , will decrease enabling higher charging current until the rectifier voltage resumes 0.9 V. When the  $V_{rec}$  is lower than 0.9 V,  $V_{g6}$  will be close to  $V_{rec}$  due to the feedback loop, and  $M_6$  thus shuts off. As the voltage on  $C_s$ ,  $V_c$ , exceeds 0.9 V, transistor  $M_6$  is kept fully on and  $V_c$  is equal to  $V_{rec}$ .

#### C. Control Logic

The control logic of the EH is shown in Figure 3. Output voltage of the rectifier is sensed by two PMOS-diode based voltage dividers,  $R_1$ - $R_2$  and  $R_3$ - $R_4$ .  $R_1$ - $R_2$  voltage divider comprises of 5 and 2 PMOS-diode connected transistors, while  $R_3$ - $R_4$  voltage divider comprises of 5 and 3 PMOS-diode connected transistors. The two-stage continuous-time comparator is implemented for the comparison of the rectifier output voltage and the reference voltage,  $V_{ref}$ . Control signal P, a result of comparison of the output voltage of the envelope detector in the demodulator with the reference voltage corresponding to the power threshold  $P_{th}$ , is input to the the control logic.

# D. Demodulator

A demodulator based on the envelope detector is inherent receiver of the passive backscattering device like RF tag. In the proposed implementation, envelope detector is implemented using 3-stage rectifier, while a comparator is added in order to determine the input power level, as shown in Figure 1. The

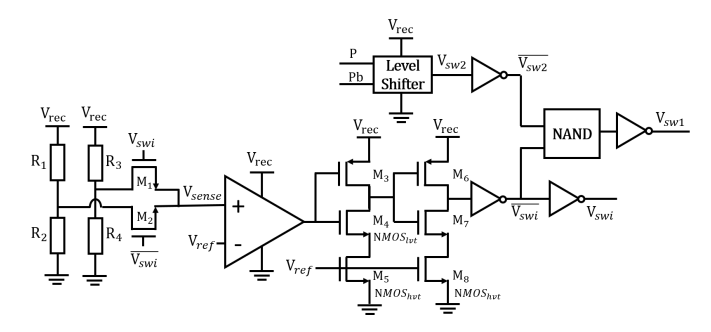


Fig. 3. Implementation of the control logic.

comparator implementation is the same as in the control logic. The output of the comparator is fed into the control logic.

# IV. SIMULATION RESULTS

The energy harvester has been implemented in 65 nm CMOS technology. To demonstrate the operation of the proposed harvester and characterize the performance, simulations have been performed at 915 MHz operating frequency.

We first demonstrate the choice of the topology of the reconfigurable rectifier. With only a storage capacitor and a  $100~\mathrm{M}\Omega$  resistor at the output of the rectifier, that models the load introduced by the control logic, the output voltage of the rectifier is shown in Figure 4(a). The total quiescent current of the implemented control logic is 5.5 nA. With the same input power, the 8-stage rectifier outputs a higher voltage than 2x4stage rectifier. The output of 8-stage rectifier reaches 1.2 V when the input power is -34 dBm and this is the minimum power at which capacitor can be fully charged when the system operates in the low-power regime. However, in the highpower regime of operation, with the increased load, 2x4-stage rectifier reaches the minimum voltage at which LDO provides supply voltage for the tag operation at input power of -26 dBm, as shown in Figure 4(b) for  $R_L$  of 0.5 M $\Omega$ . Additionally, 2x4stage rectifier has a significantly higher efficiency with this load than 8-stage rectifier.

We next demonstrate the functionality and performance of the ACC in the high-power regime operation of the harvester over a wide range of load resistances at the output of LDO. The total power consumption of the ACC is 12 nW at supply voltage of 0.9 V. The DC gain, bandwidth and unity gain frequency of the error amplifier are 30.8 dB, 116 kHz, and 3.8 MHz, respectively. Figure 5 shows the output voltage of the rectifier for different load resistors. We observe that when the storage capacitor  $C_s$  is charged through ACC, the output voltage of the rectifier is regulated to 0.91 V as the input power increases due to adapted rectifier output current and excess energy storage into  $C_s$ . We define the power conversion efficiency(PCE) of the system as:

$$PCE = \frac{V_{rec}I_{ch} + V_{LDO}^2/R_L}{P_{in}},$$
(1)

where  $I_{ch}$  is the charging current of the capacitor  $C_S$  and  $V_{LDO}$  is the output voltage of LDO regulator. In (1), the

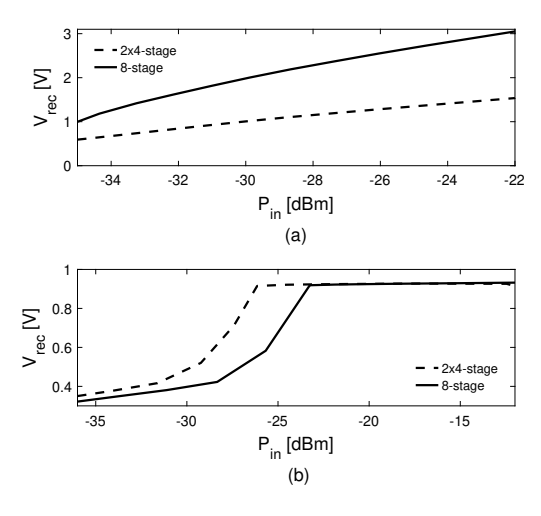


Fig. 4. Output voltage of the reconfigurable rectifier in two configurations when the load is (a) 100 M $\Omega$  resistor and (b) ACC and LDO with 0.5 M $\Omega$  load resistance  $R_L$ .

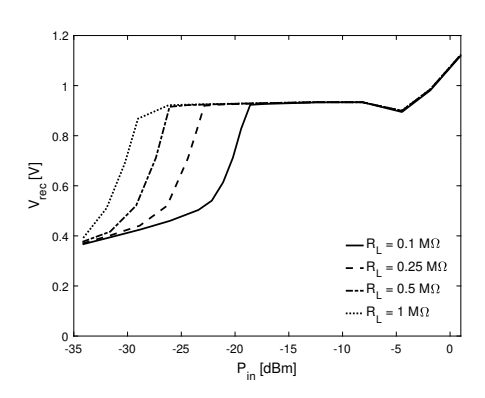


Fig. 5. Output voltage of the rectifier as a function input power with ACC at different load resistances  $R_L$ .

power loss on the transistor  $M_6$  of ACC is excluded from the dissipated power. ACC enables high power efficiency over a wide range of input power as the efficiency of the rectifier and LDO is maintained by limiting the output voltage of the rectifier, while the extra power is stored on the storage capacitor, as shown in Figure 6(b). As a reference, PCE of a system comprising rectifier and LDO without ACC is shown in Figure 6(a). Simulations also confirm that with ACC there is a very small input impedance variation for a different load resistance  $R_L$ .

We then demonstrate the functionality of the energy harvester in time as it operates in different states. First, Figure 7(a) shows that during the start-up control logic functions properly as  $V_{rec}$  reaches 0.35 V. Storage capacitor  $C_s$  is 100 pF in the simulation. As the input power reaches -34.4 dBm, the output voltage of the rectifier is 1.2 V and LDO is connected to the output of the rectifier. As the output voltage reaches  $V_{th1}$ , the LDO is disconnected and the capacitor is charged again.

Next, we simulate the operation of the harvester for two input voltages, where harvester operates in the low-power regime for one input and in the high-power regime for the second one. The storage capacitor is 1 nF in this simulation.

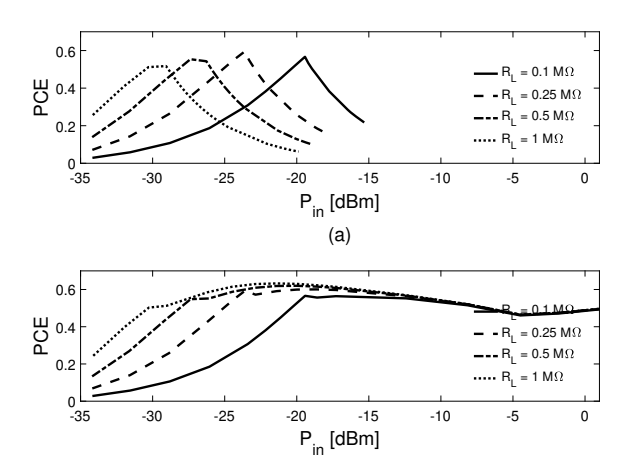


Fig. 6. PCE of the system as a function input power (a) without ACC and (b) with ACC at different load resistances.

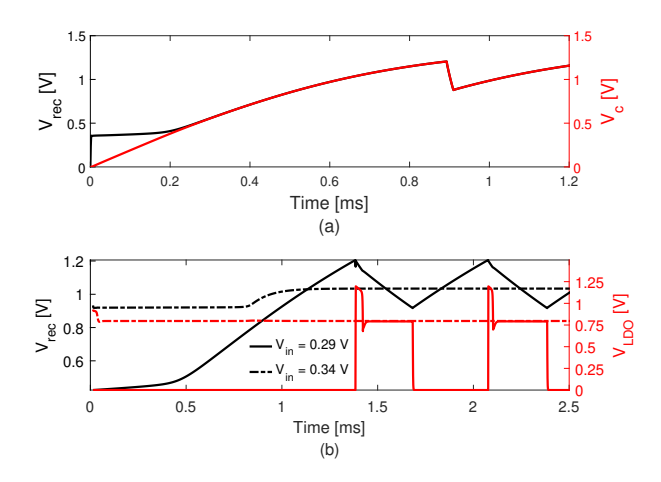


Fig. 7. (a) Output voltage of rectifier and capacitor voltage for with input voltage of  $V_{in}$ =0.225 V and (b) Output voltage of rectifier and LDO for two different values of  $V_{in}$ .

Figure 7(b) show how the harvester is cycling between State 1 and State 2 in the low-power regime and that LDO outputs a 0.8 V supply voltage when harvester is in State 2. When the harvester operates in the high-power regime, the output voltage of the rectifier reaches the minimum output voltage for the operation of LDO after the charging time of 10  $\mu$ s. During that time, transistor  $M_6$  of ACC is off and the only load at the output of the rectifier is LDO.

# V. CONCLUSION

We present an energy harvesting circuit along with the power management strategy that optimizes energy efficiency of near-zero power passive devices, like backscattering based RF tags. RF tag can operate at -34.4 dBm in a listening mode, while storage of excess energy enables performance of complex computational tasks on the tag that are critical in applications like smart spaces.

# ACKNOWLEDGMENT

This research was supported by the National Science Foundation under grant number CNS-1763843 and CNS-1901182.

#### REFERENCES

- [1] N. M. Pletcher, S. Gambini, and J. Rabaey, "A 52 muw wake-up receiver with -72 dbm sensitivity using an uncertain-if architecture," *IEEE Journal of solid-state circuits*, vol. 44, no. 1, pp. 269–280, 2009.
- [2] X. Huang, P. Harpe, G. Dolmans, H. de Groot, and J. R. Long, "A 780–950 mhz, 64–146 μw power-scalable synchronized-switching ook receiver for wireless event-driven applications," *IEEE Journal of Solid-State Circuits*, vol. 49, no. 5, pp. 1135–1147, 2014.
- [3] E. Nilsson and C. Svensson, "Power consumption of integrated low-power receivers," *IEEE Journal on Emerging and Selected Topics in Circuits and Systems*, vol. 4, no. 3, pp. 273–283, 2014.
- [4] J. Blanckenstein, J. Klaue, and H. Karl, "A survey of low-power transceivers and their applications," *IEEE Circuits and Systems Mag*azine, vol. 15, no. 3, pp. 6–17, 2015.
- [5] D. C. Daly and A. P. Chandrakasan, "An energy-efficient ook transceiver for wireless sensor networks," *IEEE Journal of Solid-State Circuits*, vol. 42, no. 5, pp. 1003–1011, 2007.
- [6] X. Lu, P. Wang, D. Niyato, D. Kim, and Z. Han, "Wireless networks with rf energy harvesting: A contemporary survey," *IEEE Communications* Surveys & Tutorials, vol. 17, no. 2, pp. 757–789, 2015.
- [7] S. Sudevalayam and P. Kulkarni, "Energy harvesting sensor nodes: Survey and implications," *IEEE Communications Surveys & Tutorials*, vol. 13, no. 3, pp. 443–461, 2011.
- [8] S. S. Reddy and C. Murthy, "Dual-stage power management algorithms for energy harvesting sensors," *IEEE Transactions on Wireless Communications*, vol. 11, no. 4, pp. 1434–1445, 2012.
- [9] F. Simjee and P. H. Chou, "Everlast: long-life, supercapacitor-operated wireless sensor node," in *Low Power Electronics and Design*, 2006. ISLPED'06. Proceedings of the 2006 International Symposium on. IEEE, 2006, pp. 197–202.
- [10] C. Park and P. H. Chou, "Ambimax: Autonomous energy harvesting platform for multi-supply wireless sensor nodes," in *Sensor and Ad Hoc Communications and Networks*, 2006. SECON'06. 2006 3rd Annual IEEE Communications Society on, vol. 1. IEEE, 2006, pp. 168–177.
- [11] C. Moser, L. Thiele, D. Brunelli, and L. Benini, "Adaptive power management in energy harvesting systems," in *Proceedings of the conference on Design, automation and test in Europe*. EDA Consortium, 2007, pp. 773–778.
- [12] V. Liu, A. Parks, V. Talla, S. Gollakota, D. Wetherall, and J. R. Smith, "Ambient backscatter: Wireless communication out of thin air," ACM SIGCOMM Computer Communication Review, vol. 43, no. 4, pp. 39– 50, 2013.
- [13] D. J. Yeager, A. P. Sample, and J. R. Smith, "Wisp: A passively powered uhf rfid tag with sensing and computation," in *RFID Handbook*. CRC Press, 2017, pp. 261–276.
- [14] J. Ryoo, J. Jian, A. Athalye, S. R. Das, and M. Stanaćević, "Design and evaluation of "bttn": A backscattering tag-to-tag network," *IEEE Internet of Things Journal*, vol. 5, no. 4, pp. 2844–2855, 2018.
- [15] J. Ryoo, Y. Karimi, A. Athalye, M. Stanaćević, S. R. Das, and P. Djurić, "Barnet: Towards activity recognition using passive backscattering tagto-tag network," in *Proceedings of the 16th Annual International Confer*ence on Mobile Systems, Applications, and Services, 2018, pp. 414–427.
- [16] Y. Karimi, Y. Huang, A. Athalye, S. Das, P. Djurić, and M. Stanaćević, "Passive wireless channel estimation in rf tag network," in 2019 IEEE International Symposium on Circuits and Systems (ISCAS). IEEE, 2019, pp. 1–5.
- [17] M. A. Abouzied, K. Ravichandran, and E. Sánchez-Sinencio, "A fully integrated reconfigurable self-startup rf energy-harvesting system with storage capability," *IEEE Journal of Solid-State Circuits*, vol. 52, no. 3, pp. 704–719, 2016.
- [18] S. Scorcioni, L. Larcher, and A. Bertacchini, "A reconfigurable differential cmos rf energy scavenger with 60% peak efficiency and-21 dbm sensitivity," *IEEE Microwave and Wireless Components Letters*, vol. 23, no. 3, pp. 155–157, 2013.
- [19] M. Stoopman, S. Keyrouz, H. Visser, K. Philips, and W. Serdijn, "Co-design of a cmos rectifier and small loop antenna for highly sensitive rf energy harvesters," *IEEE Journal of Solid-State Circuits*, vol. 49, no. 3, pp. 622–634, 2014.
- [20]  $\overline{X}$ . Hua and R. Harjani, "A  $5\mu$ w-5mw input power range, 0–3.5 v output voltage range rf energy harvester with power-estimator-enhanced mppt controller," in 2018 IEEE custom integrated circuits conference (CICC). IEEE, 2018, pp. 1–4.

- [21] M. H. Ouda, M. Arsalan, L. Marnat, A. Shamim, and K. N. Salama, "5.2-ghz rf power harvester in 0.18-/spl mu/m cmos for implantable intraocular pressure monitoring," *IEEE Transactions on Microwave Theory and Techniques*, vol. 61, no. 5, pp. 2177–2184, 2013.
- [22] M. Seok, G. Kim, D. Blaauw, and D. Sylvester, "A portable 2-transistor picowatt temperature-compensated voltage reference operating at 0.5 v," *IEEE Journal of Solid-State Circuits*, vol. 47, no. 10, pp. 2534–2545, 2012
- [23] Y. Lu, H. Dai, M. Huang, M. K. Law, S. W. Sin, S. P. U, and R. P. Martins, "A wide input range dual-path cmos rectifier for rf energy harvesting," *IEEE Transactions on Circuits and Systems II: Express Briefs*, vol. 64, no. 2, pp. 166–170, Feb 2017.
- [24] Z. Zeng, S. Shen, X. Zhong, X. Li, C.-Y. Tsui, A. Bermak, R. Murch, and E. Sánchez-Sinencio, "Design of sub-gigahertz reconfigurable rf energy harvester from- 22 to 4 dbm with 99.8% peak mppt power efficiency," *IEEE Journal of Solid-State Circuits*, vol. 54, no. 9, pp. 2601–2613, 2019.